



HAL
open science

Template directed synthesis of half condensed Schiff base complexes of Cu(II) and Co(III): Structural and magnetic studies

Priyanka Pandey, Abhineet Verma, Kateryna Bretosh, Jean-Pascal Sutter, Sailaja Sunkari

► **To cite this version:**

Priyanka Pandey, Abhineet Verma, Kateryna Bretosh, Jean-Pascal Sutter, Sailaja Sunkari. Template directed synthesis of half condensed Schiff base complexes of Cu(II) and Co(III): Structural and magnetic studies. *Polyhedron*, 2019, 164, pp.80-89. 10.1016/j.poly.2019.02.037 . hal-02140510

HAL Id: hal-02140510

<https://hal.science/hal-02140510v1>

Submitted on 10 Nov 2020

HAL is a multi-disciplinary open access archive for the deposit and dissemination of scientific research documents, whether they are published or not. The documents may come from teaching and research institutions in France or abroad, or from public or private research centers.

L'archive ouverte pluridisciplinaire **HAL**, est destinée au dépôt et à la diffusion de documents scientifiques de niveau recherche, publiés ou non, émanant des établissements d'enseignement et de recherche français ou étrangers, des laboratoires publics ou privés.

Template Directed Synthesis of Half Condensed Schiff base Complexes of Cu(II) and Co(III) : Structural and Magnetic Studies

Priyanka Pandey,^a Abhineet Verma,^a Kateryna Bretosh,^b Jean-Pascal Sutter^b and Sailaja S. Sunkari^{*:a}

^aDepartment of Chemistry, Mahila Mahavidyalay, Banaras Hindu University, Varanasi 221 005, India

^bLCC-CNRS, Université de Toulouse, CNRS, Toulouse, France

Abstract

By proper choice of substituents on the aldehyde and amine, the nature of Schiff base formed (fully condensed or half condensed) could be tuned by the templating effect of the metal ion. Condensation of 5-chlorosalicylaldehyde with ethylene diamine in the presence of Co(II) or Cu(II) and azido anions have afforded two new half condensed Schiff base metal complexes $[\text{CuL}(\mu\text{-}1,1\text{-N}_3)]_2$ (**1**) and $[\text{CoL}_2]\text{N}_3\cdot\text{H}_2\text{O}$ (**2**), where L = (E)-2-((2-aminoethyl)methyl)-4-chlorophenol that were structurally characterized by X-ray analysis, IR and UV spectra. Complex **1** is an asymmetric $\mu\text{-}1,1$ azide bridged dimer displaying weak antiferromagnetic interactions ($J = -2.93 \pm 0.03 \text{ cm}^{-1}$), in agreement with the axial-equatorial N_3 -linkage between the two copper centers. Complex **2** is a monomer of low spin Co(III).

1. Introduction

Synthesis and structural studies of polynuclear metal complexes is well known in coordination chemistry due to its possible applications in catalysis,^[1] molecule based magnetism,^[2] sensing,^[3] DNA cleavage^[4] and so on. Among several type of ligands used, Schiff bases (SBs) are unique with their planar geometry providing four or three coordination sites depending on the type of condensation product, viz., a fully condensed SB or a half condensed SB.^[5] The planarity imposed by the fully condensed Schiff base ligands is well suited for encapsulating the metal ions into the cavity of the ligating phenoxo oxygen and imino nitrogen atoms, there by leaving the axial positions of a typical metal ion with octahedral geometry free, allowing for

coordination to other ligating species. Depending on the synthetic conditions as well as the geometry and ligating characteristics of auxiliary ligands, such attempts led to the formation of discrete^[6] or polymeric/network structures.^[7] A close look at reported Schiff base complexes reveals that the formation of a fully or half condensed Schiff base appears to be directed by the symmetry of the amine,^[8] nature of substituents on the amino N,^[9] orientation of the amino group with respect to the substituent groups present on the carbon to which amino N is attached^[10] and the variations in the donor capability of the N lone pair due to its involvement in the conjugation with available double bonds.^[11] Irrespective of the molar ratios, a conformationally free symmetric amine, having bulky groups that restrict the free rotation of amino group leads to a fully condensed Schiff base that may be isolated. In the absence of conditions that lead to a fully condensed Schiff base, as described above, isolation of a half condensed Schiff base with a symmetric amine is possible only under the templating effect of a metal ion.^[12] Such isolated complexes of half condensed Schiff bases have been found with Cu(II)^[13] and Ni(II)^[8a,14] directed by the anions like azide, cyanate, thiocyanate, dicyanamide.

In the context of magneto chemistry, literature is saturated with numerous examples of fully condensed Schiff base metal complexes, especially copper complexes that helped establish magneto structural correlations.^[15] Among the auxiliary ligands, azides are unique with reference to their bridging modes in Cu(II) complexes, thus generating a plethora of structures of relevance in magneto chemistry.^[16] Such systems provide ideal test systems for understanding the basics of magnetic interactions in extended systems.^[17] Previously we too have demonstrated the formation of tetranuclear clusters of Cu(II) involving salpn/salophen as SB and azide as an auxiliary ligand.^[18] However, change in the aldehyde component of the schiff base from a simple aldehyde to a chloro substitution at the fifth position led to the formation of half condensed Schiff bases templated by the metal ion. The numbers of half condensed Schiff base complexes are still limited compared to their fully condensed counterparts. Contrary to the fully condensed Schiff base complexes with predefined geometrical constraints, half condensed Schiff base complexes with their tridentate coordination capabilities can generate versatile structures with modified coordination geometries which may be helpful in changing the electronic structure of the metal ion leading to desired magnetic behavior, depending on the metal ion, auxiliary ligands and synthetic conditions. Sparsely reported examples include Fe(III) complexes of halogenated quinolyl salicylaldimines with SCN⁻^[19] and pseudo halide bridged dinuclear copper(II)

complexes with naphthaldehyde and substituted diamines^[20] Highlighting the potential of half condensed Schiff base complexes in generating structurally rich systems of magnetic relevance, and a means to deliberately synthesize them, herein we report the synthesis and structure of Cu(II) and Co(III) complexes involving half condensed schiff base (E)-2-((2-aminoethyl)methyl)-4-chlorophenol (L) and azide along with the magnetic properties of the Cu(II) complex **2**.

2. Experimental Section:

2.1 Materials and Instrumentation:

Cu(CH₃COO)₂·H₂O, Co(CH₃COO)₂·4H₂O, ethylenediamine and 5-chlorosalicylaldehyde were purchased from Sigma Aldrich chemicals. Infrared spectra were recorded on a Perkin Elmer FTIR spectrometer, Spectrum-2 as KBr pellets in the region 400-4000 cm⁻¹. Elemental analyses were done on a CE-40 elemental analyzer for both the complexes. Electronic spectra were recorded on a CARY 100 BIO UV-Visible Spectrophotometer. Variable-temperature dc susceptibility measurements were performed on a Quantum Design MPMS-5 SQUID magnetometer. Diamagnetic corrections were applied for the compounds' constituent atoms by using Pascal's constants and for the sample holder. Cyclic voltammogram of **2** was recorded with Auto lab (PG STAT, 302, The Netherlands, NOVA 1.11 software) using a conventional three-electrode system.

Caution: Azide as well as their metal complexes are potentially explosive and should be handled with great care and in small quantities.

2.2 Synthesis

2.2.1. Synthesis of the complexes

2.2.1.1. [CuL(μ_{1,1}-N₃)₂] (**1**): To 10 mL methanolic solution of 5-chlorosalicylaldehyde (0.328 g, 2.00 mmol), ethylene diamine (80.00 μL, 1.00 mmol) was added drop by drop and stirred for 10 minutes. To this solution 10 mL methanolic solution of Cu(CH₃COO)₂·H₂O (0.400 g, 2.00 mmol) was added drop by drop under stirring and stirring continued for 15 minutes, followed by the addition of 7 mL methanolic solution of NaN₃ (0.120 g, 2.00 mmol). Then, the entire mixture was refluxed at 60°C for 3 hour under continuous stirring. X-ray quality crystals were obtained within 6-7 days from slow evaporation of mother liquor at room temperature (35°C).

Yield: 0.208 g (67.75 %, 0.68 mmol), M.P. = 273 (\pm 1) °C. Analysis Calculated (found) for $C_{18}H_{20}N_{10}O_2Cl_2Cu_2$: C, 35.65 (35.53); H, 3.32 (3.37); N, 23.10 (23.14) %. FT-IR (cm^{-1}): 3293(br), 3213(w), 3126(w), 2921(w), 2851(w), 2038(s), 1651(s), 1639(s), 1588(s), 1457(s), 1368(m), 1310(s), 1175(s), 1132(m), 1049(s), 837(s), 704(s), 655(m), 459(m).

2.2.1.2. $[CoL_2]N_3 \cdot H_2O$ (**2**): To 7 mL methanolic solution of 5-chlorosalicylaldehyde (0.116 g, 0.74 mmol), ethylene diamine (26.00 μ L, 0.37 mmol) was added drop by drop resulting in a yellow solution. Then 5 mL aqueous solution of $Co(CH_3COO)_2 \cdot 2H_2O$ (0.093 g, 0.37 mmol) was added to it drop by drop with continuous stirring, resulting in the formation of a brown precipitate, followed by 5 mL aqueous solution of NaN_3 (0.048 g, 0.74 mmol). The whole contents were transferred to a 25 mL Teflon reactor and heated at 500°C for 5 hours under autogenous pressure. Subsequently, the vessel was cooled to room temperature. Small amount of precipitate formed was removed by filtration and the clear blood red filtrate was left at RT (35°C), from which X-ray quality red block shaped crystals were obtained within 2-3 days.

Yield: 0.140 g (74.20 %, 0.27 mmol), M.P. = 241 (\pm 1) °C. Analysis Calculated (found) for $C_{18}H_{18}N_7O_3Cl_2Co$: C, 42.37 (42.53); H, 3.56 (3.47); N, 19.22 (19.14) %. FT-IR(cm^{-1}): 3197(br), 3102(w), 2956(w), 2922(w), 2036(s), 1646(s), 1596(s), 1460(s), 1375(m), 1306(s), 1148(m), 1133(s), 1064(s), 830(m), 702(s), 628(m), 484(m).

2.3. X-ray Crystallography:

Crystal data for the complex **1** was collected on a Saturn 724 (4x4 bin mode) at 77 K and for **2** on a Bruker APEX-II CCD diffractometer using graphite monochromatized Mo Ka radiation at 298 K ($\lambda = 0.71073 \text{ \AA}$). The data of **1** was reduced by using 'CrystalClear (Rigaku/MSI Inc., 2006) and for complex **2** was reduced by using Bruker SAINT. The structures were solved by direct methods and refined by full matrix least squares on F^2 using SHELX-2016.^[21] The non-hydrogen atoms were refined with anisotropic thermal parameters. All the ring hydrogen atoms were geometrically fixed and allowed to refine using a riding model. Water hydrogens for **2** were located from difference maps and their positions refined by DFIX while thermal parameters were refined using a riding model. The refinement converged to a final $R1 = 0.0260$; $wR2 = 0.0664$ for **1** and $wR2 = 0.0353$, $wR2 = 0.0972$ for **2**. Important crystal data are presented in Table 1 and

selected inter-atomic distances and angles in Table 2. Drawings were made using ORTEP-III^[22] and Mercury.^[23]

Table 1. Important Crystallographic data for complexes **1** and **2**.

	1	2
Formula	C ₁₈ H ₂₀ N ₁₀ O ₂ Cl ₂ Cu ₂	C ₁₈ H ₁₈ N ₇ O ₃ Cl ₂ Co
Fw	303.21	510.22
Crystal system	Triclinic	Monoclinic
Space group	P $\bar{1}$	P2 ₁ /c
<i>a</i> (Å)	5.7113(19)	9.8998(4)
<i>b</i> (Å)	8.463(3)	22.2831(10)
<i>c</i> (Å)	11.860(4)	10.4143(5)
α (°)	77.118(7)	90
β (°)	86.469(11)	114.507(1)
γ (°)	80.549(10)	90
<i>V</i> (Å ³)	551.1(3)	2090.41(16)
<i>Z</i>	2	4
F(000)	306	1040
μ (mm ⁻¹)	2.213	1.113
ρ (g cm ⁻³)	1.827	1.621
R _{int}	0.0311	0.0449
R [I > 2 σ (I)]	0.0260	0.0353
wR2 [I > 2 σ (I)]	0.0664	0.0972

R (all data)	0.0313	0.0413
wR2 (all data)	0.0680	0.1006
GoF	1.009	1.076
λ (Å)	0.71073	0.71073

$$R1 = \Sigma||F_o|-|F_c|/\Sigma|F_o|; wR2 = [\Sigma w(|F_o|^2-|F_c|^2)^2 / \Sigma w|F_o|^2]^{1/2}.$$

2.4. Hirshfeld surface analysis

Molecular Hirshfeld surfaces in the crystal structure are examined on the basis of the electron distribution calculated as the sum of spherical atom electron densities. The Hirshfeld surfaces are mapped with d_{norm} , the normalized contact distance based on both d_e (the distance from the point to the nearest nucleus external to the surface) and d_i (the distance to the nearest nucleus internal to the surface) and the van der Waals (vdW) radii of the atom, given by equation (1). The value of d_{norm} is negative or positive depending on intermolecular contacts being shorter or longer than the van der Waals separations. Hirshfeld surface and associated 2D fingerprint plots were calculated using CrystalExplorer 2.1.30.^[24] The 2D plots were created by binning (d_e , d_i) pairs in intervals of 0.01 Å and coloring each bin (essentially a pixel) of the resulting 2D histogram, as a function of the fraction of surface points in that bin, ranging from blue (few points) through green to red (many points). Graphical plots of the molecular Hirshfeld surfaces were mapped with d_{norm} using a red–white–blue color scheme, where red highlights shorter contacts, white for contacts around the vdW separation, and blue for longer contacts.

$$d_{\text{norm}} = [(d_i - r_i^{\text{vdW}}) / r_i^{\text{vdW}}] + [(d_e - r_e^{\text{vdW}}) / r_e^{\text{vdW}}] \quad (1)$$

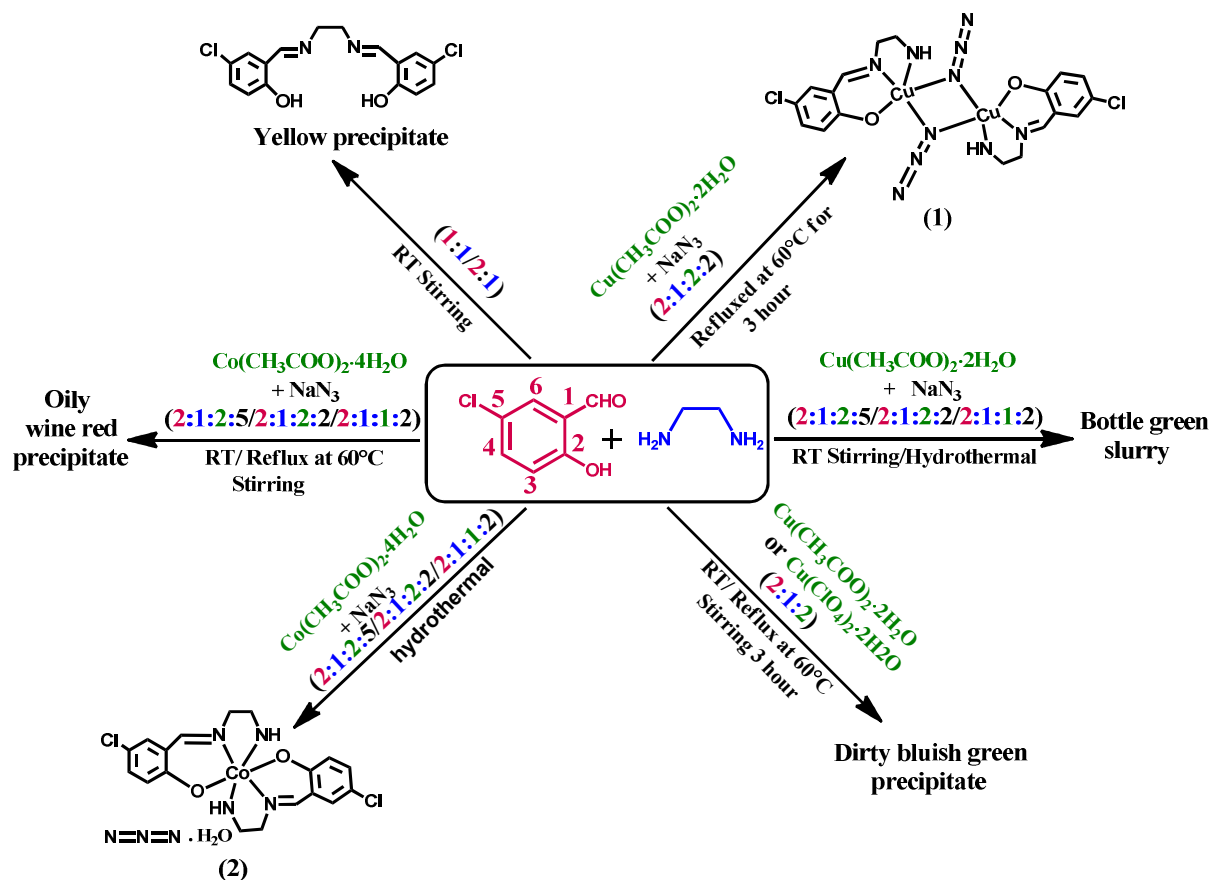
3. Results and discussion

3.1. Synthesis & IR spectra

Both the complexes **1** and **2** were obtained in moderately good yields by the self assembly of the aldehyde, amine, metal and anion in 2:1:2:2 molar ratios, without prior isolation of the ligand. However, reacting only amine and aldehyde in either 1:1 or 1:2 ratios always yielded a fully

condensed Schiff base (Scheme 1). In both the complexes, half condensed schiff base product was obtained, inspite of the available molar ratios of aldehyde and amine for the formation of a fully condensed Schiff base. This may be attributed to the templating effect of the metal ion directed by azide, which stabilizes a square pyramidal copper with three coordinating sites occupied by the half condensed Schiff base and the remaining two sites by asymmetrically bridging azide. Several such half condensed Schiff base complexes of copper with azide, cyanate, thiocyanate were also reported previously by reacting aldehyde and amine in 1:1 molar ratios.^[25] However, we have not come across any reports of half condensed Schiff bases, inspite of available molar ratios of 1:2 for amine and aldehydes.

Complex **1** was formed under reflux at 60°C and **2** under hydrothermal conditions. In case of **1**, refluxing of the solution yields crystals from mother liquor. If not refluxed, a highly insoluble precipitate forms by room temperature stirring of the components which could not be further crystallized. Reaction with preformed Schiff base, Cu(II) and azide either by simple stirring or refluxing also yields a green slurry which could not be characterized further. In case of **2**, gel like precipitate formation takes place at either room temperature stirring or under reflux conditions. Only heating under pressure afforded crystals of the compound **2**. Further, it has been observed that varying the aldehyde, amine, metal and anion molar ratios from 2:1:1:1/2:1:1:2/2:1:2:2/2:1:2:5 always afforded only **2**; while in case of **1**, variation of aldehyde, amine, metal and anion ratios from 2:1:1:1/2:1:1:2/2:1:2:5 resulted in dirty green slurry formation which could not be further crystallized. Scheme 1 summarizes the reaction conditions and products formed.



Scheme 1: Summary of synthetic conditions favoring formation of **1** and **2**.

IR (cm^{-1}) spectra of the complex shows absorption peaks in the range of $3293\text{-}2851\text{ cm}^{-1}$ which are assigned to $\nu_{\text{as}}(\text{N-H})$ of the schiff base indicating the presence of amine (Figure S1). Imine ($\text{C}=\text{N}$) stretching frequency occurs between $1645\text{ to }1655\text{ cm}^{-1}$ while peaks at the 2038 cm^{-1} correspond to $\mu\text{-}1,1$ bridging mode of the azido anions and peaks at 2086 cm^{-1} corresponds to the free azide.^[26]

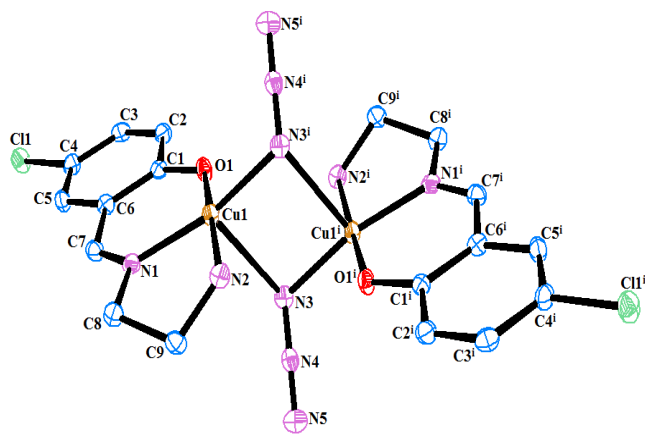
Table 2. Selected bond lengths (Å) and angles (°) for **1** and **2**.

1			
Bond lengths (Å)			
Cu(1)-Cu(1)#1	3.1593(11)	Cu(1)-N(3)	2.001(2)
Cu(1)-O(1)	1.920(2)	Cu(1)-N(2)	2.005(2)
Cu(1)-N(1)	1.949(2)	Cu(1)-N(3)#1	2.470(2)
Bond Angle (°)			
Cu(1)-N(3)-Cu(1)#1	89.30(8)	N(1)-Cu(1)-N(2)	84.81(8)
O(1)-Cu(1)-N(1)	93.39(8)	O(1)-Cu(1)-N(2)	174.28(8)
N(1)-Cu(1)-N(3)	164.08(8)	O(1)-Cu(1)-N(3)	90.86(7)
2			
Bond lengths (Å)			
Co-O(1)	1.8930(16)	Co-N(4)	1.9068(19)
Co-O(2)	1.8932(16)	Co-N(2)	1.950(2)
Co-N(1)	1.9004(19)	Co-N(3)	1.954(2)
Bond Angle (°)			
O(1)-Co-O(2)	91.30(7)	O(2)-Co-N(4)	94.23(8)
O(1)-Co-N(1)	94.93(8)	N(1)-Co-N(4)	177.40(8)
O(2)-Co-N(1)	87.51(7)	O(1)-Co-N(2)	179.25(8)
O(1)-Co-N(4)	86.97(7)	HW(1A)-OW(1)-HW(1B)	103(2)

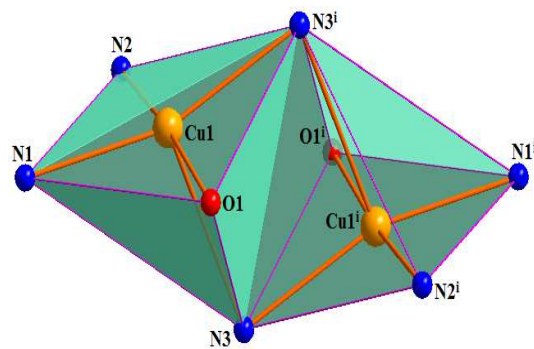
Symmetry transformations used to generate equivalent atoms: #1 -x,-y+2,-z+1 for **1**.

3.2 . Crystal Structure Description

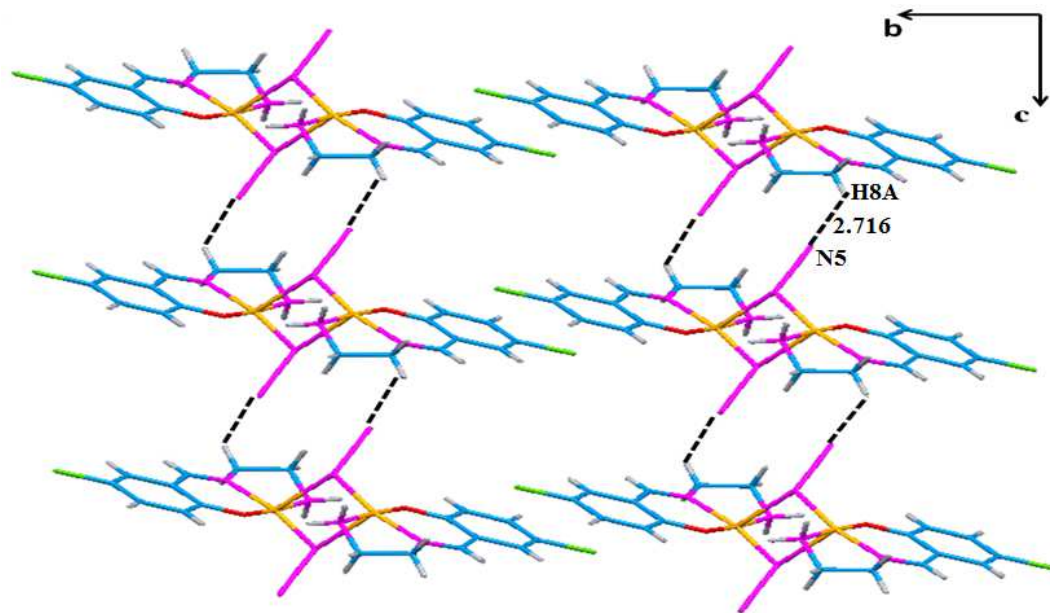
3.2.1. Structure of [Cu(L)(N₃)₂](1): **1** crystallizes in the triclinic space group P $\bar{1}$. Cu(II) is in a square pyramidal arrangement with the ligand nitrogens (N1 and N2), phenoxo oxygen (O1) and azide nitrogen (N3) occupying the base of the pyramid and symmetry related azido N (N3[′]) occupying the apex of the pyramid (Figure. 1a and b). Cu deviates by ~ 0.1 Å from the square plane. Azide acts as asymmetric μ -1,1 bridge and connects Cu1 to its inversion related unit. Both the Cu centers within the dimer are separated by 3.1593(11) Å. Crystal packing (Figure 1c and 1d) is stabilized by intramolecular C-H \cdots N (2.716 Å), N-H \cdots O (H \cdots N = 2.583 Å) and C-H \cdots Cl (H \cdots Cl = 2.885 Å) hydrogen bonding interactions (Table 3). Though asymmetrically end-on azide bridged Cu(II) dimers are plenty in reported literature, asymmetric basal-apical end-on azide bridged Cu(II) dimers with half condensed Schiff base ligands are rather limited. Among the reported dimers, the ones structurally quite close to **1** are [Cu₂L₂(N₃)₂] (L=1-(N-salicylideneamino)-2-aminoethane)^[5a] [CuL(μ -1,1-N₃)]_n where (L=4-chloro-2-[(2-dimethylaminoethylimino)methyl]phenolate)^[27], [Cu₂L₂(μ -1,1-N₃)₂]·H₂O·CH₃OH (L=1-(N-ortho-hydroxyacetophenimine)-2-aminoethane)^[25b], [Cu(L²)₂(μ -1,1-N₃)₂], where L² = N₂O half condensed Schiff base of naphthaldehyde and N,N-dimethyl diaminopropane and [Cu(L⁴)₂(μ -1,1-N₃)₂], where L⁴ = N₂O half condensed Schiff base of naphthaldehyde and N,N-diethyl diaminopropane.^[20] The coordination behavior of the ligand, Cu-N distances and angles at azide bridge in **1** are similar to these reported systems. The structural parameters relevant for magnetic discussion are tabulated in Table 4.



(a)



(b)



(c)

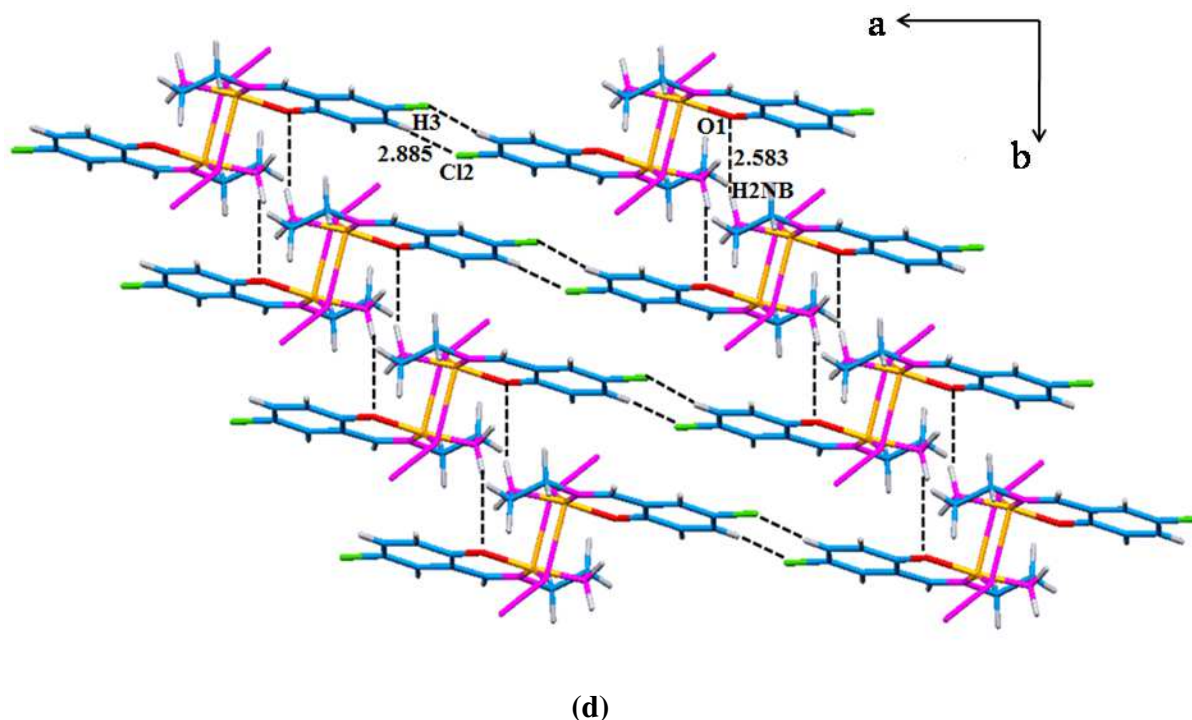
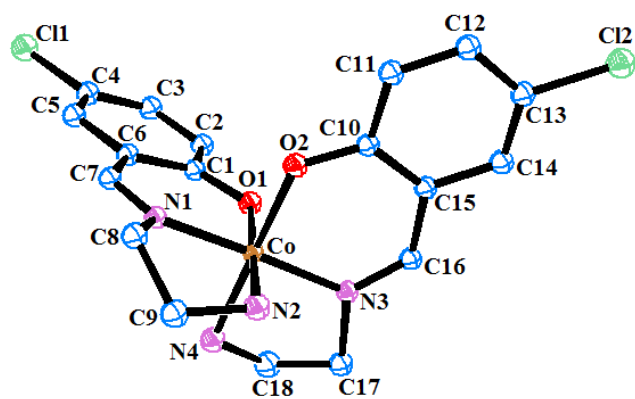


Figure 1 (a). Ortep of **1** showing atoms as 40% probability ellipsoids. Symmetry code: $i = -x, -y+2, -z+1$, **(b)** Polyhedra of Cu1 and Cu1ⁱ showing distorted square pyramidal geometry, **(c-d)** Crystal packing of **1** showing hydrogen bond interactions to form supramolecular network.

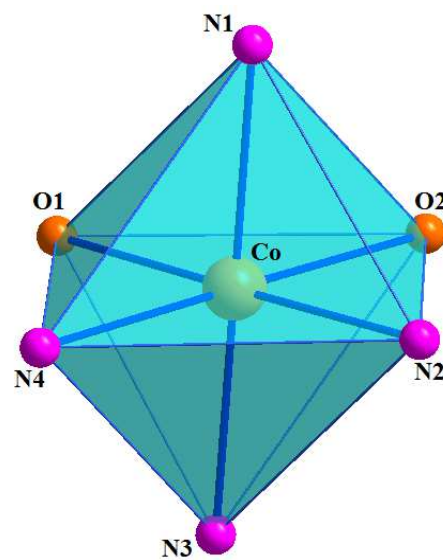
3.2.2. Structure of $[\text{Co}(\text{L})_2]\text{N}_3 \cdot \text{H}_2\text{O}$ (**2**):

Complex **2** crystallizes in monoclinic space group $P2_1/c$. Co(III) is octahedrally coordinated by two imine nitrogen's, two phenolic oxygen's and two amine nitrogens of the two Schiff base ligands (Figure 2a and 2b). Phenoxo oxygens (O1 and O2) and amine nitrogens (N2 and N4) forms base of the square plane and imino nitrogens (N1 and N3) occupy the axial positions of the octahedron. Crystal packing is shown in Figure 2c. There is one uncoordinated azide anion in the unit cell which hydrogen bonds with the solvent water hydrogens to form and stabilize the supramolecular network. The packing structure is further stabilized by C-H \cdots Cl interactions ($\text{H}\cdots\text{Cl} = 2.89\text{-}2.93 \text{ \AA}$); O-H \cdots N ($\text{H}\cdots\text{N} = 2.089\text{-}2.81 \text{ \AA}$) and N-H \cdots N ($\text{H}\cdots\text{N} = 1.929\text{-}2.201 \text{ \AA}$) interactions, propagating a 2-D network of 1-D chains formed by C-H \cdots Cl interactions (Table 3). Such weak C-H \cdots Cl interactions in the range 2.84-

2.92 Å for $\text{H}\cdots\text{Cl}$, have been previously reported in Co(III) systems^[28] and in (4-benzylpyridinium) tetrachloro cuprate(II) complex in the range, 2.42-2.78 Å.^[29]



(a)



(b)

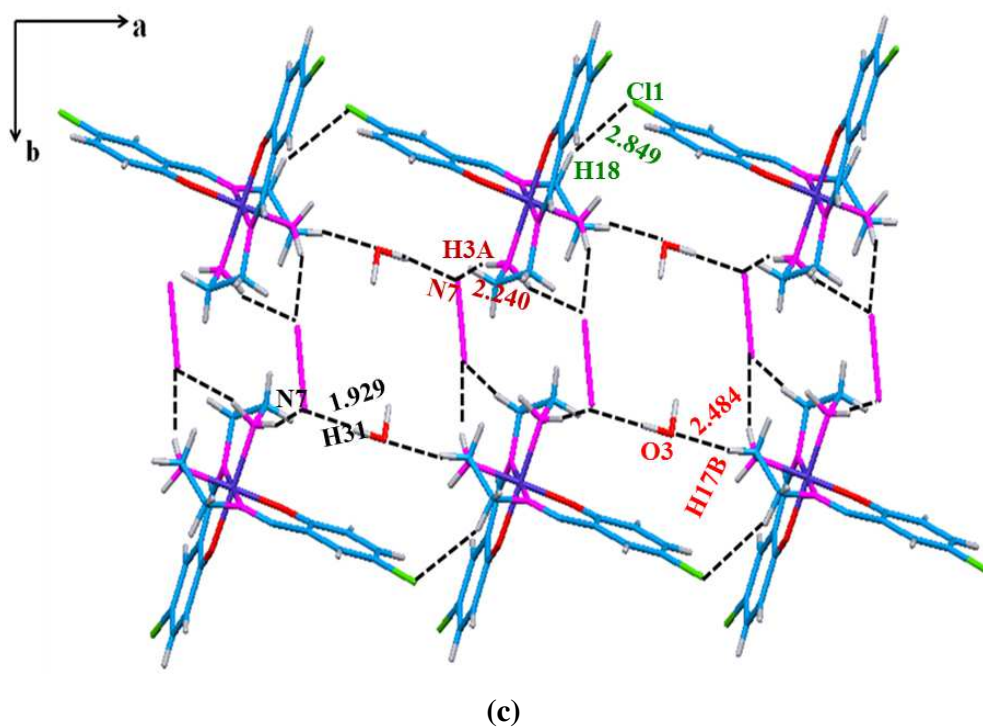


Figure 2 (a). Ortep of **2** showing atoms as 40% probability ellipsoids; solvent water and uncoordinated azide have been omitted for clarity **(b)** Polyhedra of Co(III) showing distorted Octahedral geometry; **(c)** Crystal packing of **2** showing hydrogen bonding interactions propagating supramolecular network.

Table 3. Hydrogen-bonding distances (Å) and angles (°) for complexes **1** and **2**.

Compound	D-H...A	D-H	H...A	D...A	<D-H...A
1	N(2)-H(2NB)...O(1)#2	0.89	2.58	3.449(3)	164.5
	N(2)-H(2NB)...N(3)#3	0.89	2.57	3.107(3)	119.6
	C(3)-H(3)...Cl(2)#4	0.93	2.88	3.761(3)	157.5
	C(7)-H(8)...Cl(2)#5	0.93	2.99	3.612(3)	125.8
	C(9)-H(9B)...N(4)#1	0.97	2.70	3.400(3)	129.4
2	C(3)-H(3)...OW1#1	0.93	2.55	3.291(3)	137.3
	C(7)-H(7)...O(1)#2	0.93	2.43	3.172(3)	137.1
	C(8)-H(8A)...N(5)	0.97	2.64	3.391(4)	134.6
	C(9)-H(9B)...Cl(2)#3	0.97	2.93	3.715(3)	138.8
	C(10)-H(10A)...OW1#4	0.97	2.54	3.159(3)	121.3
	C(11)-H(11B)...Cl(2)#5	0.97	2.89	3.765(3)	150.3
	C(12)-H(12)...N(7)#6	0.93	2.46	3.348(3)	161.0
	OW1-HW1A...N(6)	0.862(10)	2.81(2)	3.529(3)	142(3)
	OW1-HW1A...N(7)	0.862(10)	2.089(15)	2.926(3)	164(3)
	OW1-HW1B...Cl(1)#7	0.861(10)	2.93(3)	3.513(2)	126(3)
	OW1-HW1B...Cl(1)#2	0.861(10)	2.81(4)	3.367(2)	124(3)

Symmetry transformations used to generate equivalent atoms:

#1 -x, -y+2, -z+1; #2 x+1, y, z; #3 -x+1, -y+2, -z+1; #4 -x-2, -y+2, -z+2; #5 -x-1, -y+1, -z+2
for **1** and #1 -x, y+1/2, -z+1/2; #2 x, -y+3/2, z+1/2; #3 x, y, z+1; #4 -x, -y+1, -z+1; #5 x-1, y,
z; #6 x, y, z-1; #7 -x, y-1/2, -z+1/2 for **2**.

4. Hirshfeld surface analysis

Hirshfeld surface for both the complexes **1** and **2**, mapped over d_{norm} are shown in Figures 3a and 3b. Each molecule in the asymmetric unit of a given crystal structure have a unique Hirshfeld surface. Transparent surfaces allow visualization of the molecular moiety around which they are calculated. The red spot on the d_{norm} surface indicate hydrogen bond contacts as well as other weak interactions. Hirshfeld surface analysis provides a visual way to evaluate the percentage contribution of the various intermolecular interactions in the crystal packing. It has great influence to explore packing adaptation of crystal in a unit cell through various type of intermolecular interaction. Thus, we employed the Hirshfeld surface analysis to study such interactions present in the structure and provide a powerful tool to explain, adapting to different crystal-packing structure.^[18, 30]

Percentage contributions of various type of intermolecular interaction in fingerprint such as $\text{H}\cdots\text{H}$, $\text{C}\cdots\text{H}$, $\text{Cl}\cdots\text{H}$, $\text{N}\cdots\text{H}$, $\text{N}\cdots\text{C}$, $\text{O}\cdots\text{H}$ and $\text{C}\cdots\text{C}$, are shown as bar graph Figure 3c. The 2D fingerprint plot presented in Figure S2., provide a summary of each combination of d_e and d_i across the surface of molecule.

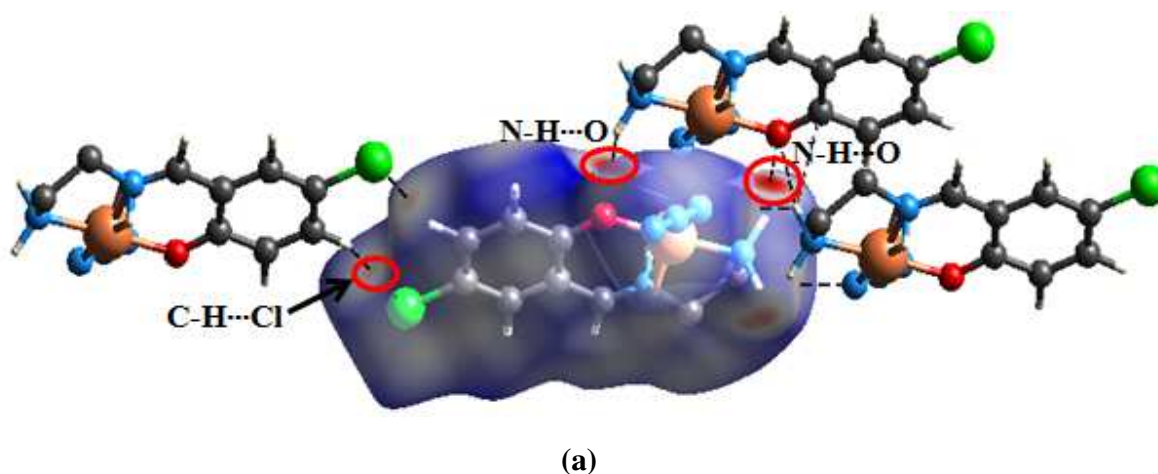
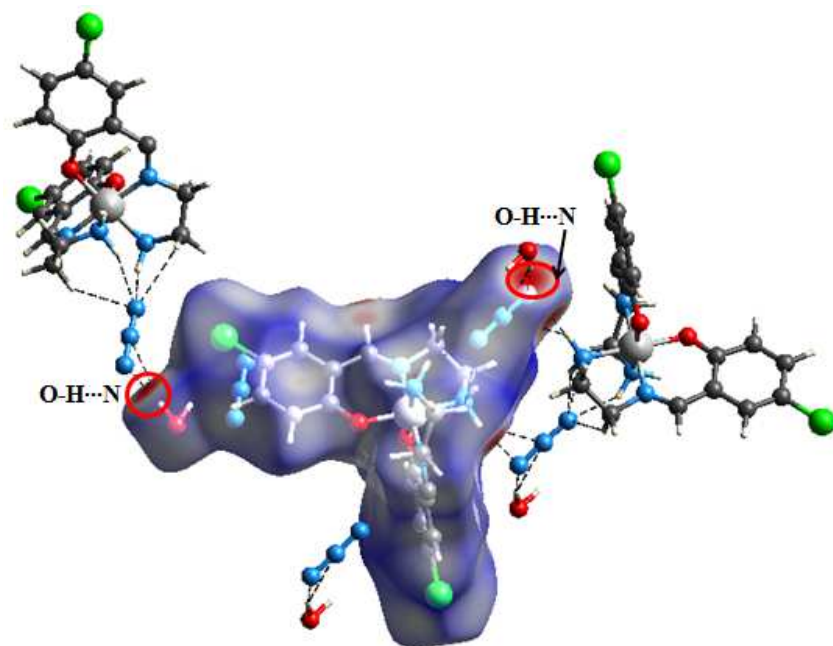
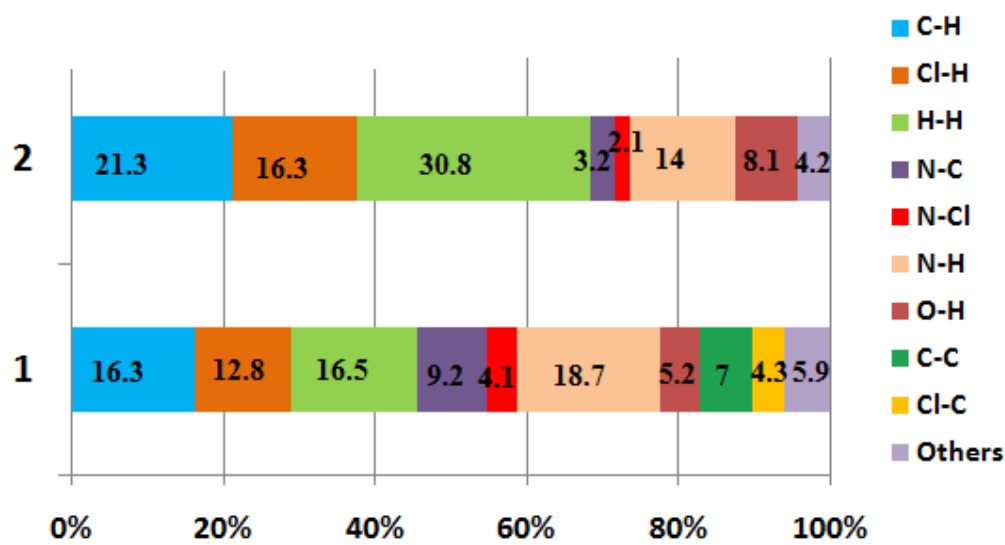


Figure 3a. Hirshfeld surface of complex **1** mapped with d_{norm} showing short range $\text{N-H}\cdots\text{O}$ and $\text{C-H}\cdots\text{Cl}$ interaction.



(b)

Figure 3b. Hirshfeld surface of complex **2** mapped with d_{norm} showing short range O-H...N interaction.



(c)

Figure 3c. Relative contributions of various intermolecular contacts to the Hirshfeld surface area in complex **1** and **2**.

5. Electronic spectra

The solution state absorption spectra for both the complexes are recorded in DMSO and presented in Figure 4. Complex **1** shows two bands, band centered between 365-420 nm (λ_{max} at 377 nm) due to ligand to ligand charge transfer (LLCT), while broad band between 530-690 nm (λ_{max} at 617 nm) are assigned to d-d transitions of the metal ion. For complex **2**, three bands were observed. Band centered between 360-490 nm (λ_{max} at 393 nm) assigned to ligand-ligand charge transfer (LLCT) while band centered between 460-530 nm (λ_{max} at 487 nm) due to ligand to metal charge transfer (LMCT). While broad band between 550-680 nm (λ_{max} at 595 nm) are assigned to d-d transitions of the metal ion.^[31]

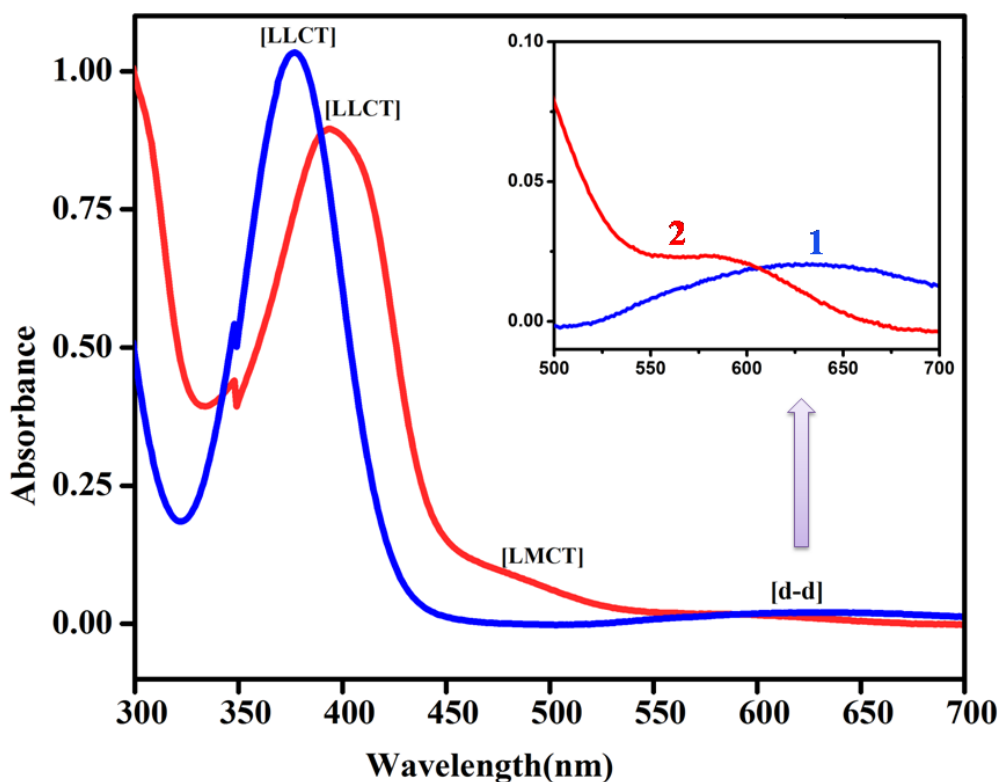


Figure 4. UV-visible spectra of complexes **1** and **2** in DMSO Solvent. (Inset) enlarged view of d-d transition band.

6. Magnetic properties

The temperature dependence for $\chi_M T$ (χ_M stands for the molar magnetic susceptibility calculated for the Cu_2 unit) found for **1** (Figure 5) is characteristic for weak antiferromagnetic interaction, in agreement with the axial-equatorial N_3 -linkage between the two centers.^[32] At 300 K, a value of $0.81 \text{ cm}^3 \text{ mol}^{-1} \text{ K}$ was found for $\chi_M T$, in agreement with the contribution of two non-interacting Cu(II) centers. This value remains unchanged as T is lowered to ca 50 K, below which temperature it rapidly decreases to reach $0.36 \text{ cm}^3 \text{ mol}^{-1} \text{ K}$ for 2 K. A Curie-Weiss analysis of $\chi_M^{-1} = f(T)$ for the susceptibility data per Cu above 20 K (Fig. S4) led to $C = 0.40 \text{ cm}^3 \text{ mol}^{-1}$ and $\theta = -0.83 \text{ K}$. Isothermal field dependence of the magnetization (Figure. 5 inset) recorded at 2, 3 and 5 K is in agreement with rather weak antiferromagnetic interaction between the Cu centers. The strength of the Cu-Cu exchange interaction was assessed by analyzing the $\chi_M T$ behavior using the Bleaney-Bowers expression for a $S = 1/2$ dimer (derived from the phenomenological Hamiltonian $H = -J\mathbf{S}_A \cdot \mathbf{S}_B$).^[33] Best fit to the experimental behavior yielded an exchange parameter of $J = -2.93 \pm 0.03 \text{ cm}^{-1}$ and $g = 2.084 \pm 0.001$ (Fig. S5). The same result was obtained when the analysis was performed simultaneously on $\chi_M T$ and the magnetization behaviors using PHI,^[34] yielding $J = -2.93 \pm 0.05 \text{ cm}^{-1}$ and $g = 2.083 \pm 0.003$. The calculated behaviors well fit to experimental data (Figure. 5) except a slight discrepancy for magnetization at 2 K. This was not improved when possible intermolecular interactions have been taken into account. These result confirm that the exchange interaction mediated by the 1,1- N_3 bridges in **1** are weak.

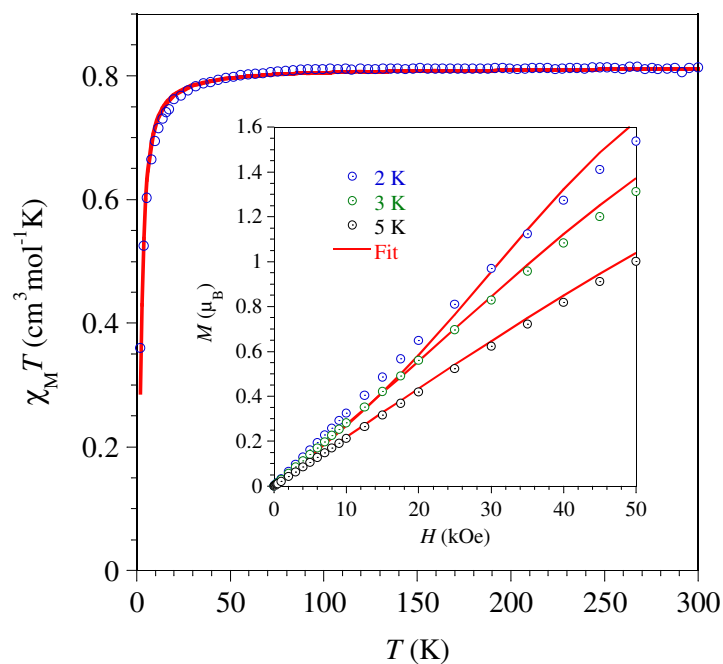
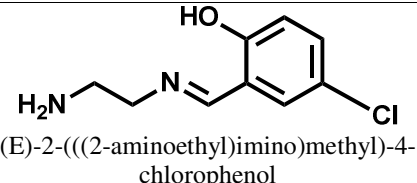
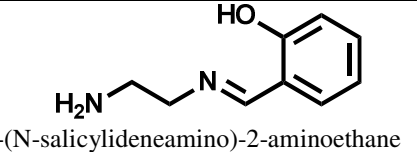
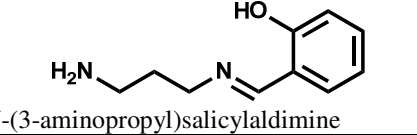
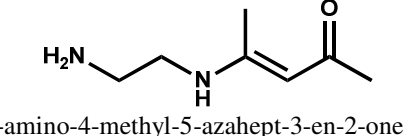
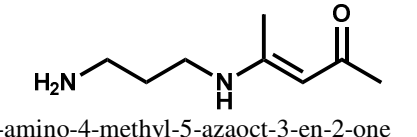
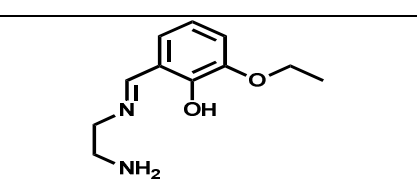


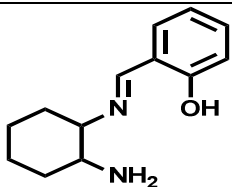
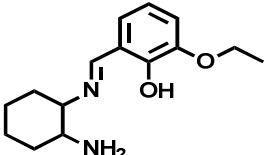
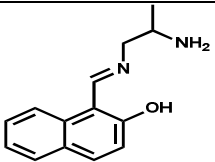
Figure 5: Experimental (\circ) and calculated ($-$) temperature dependence of $\chi_M T$ and (inset) field-dependence of the magnetization for different temperatures between 2 and 5 K; best fit parameters are discussed in main text.

Magneto-structural parameters for double $\mu_{1,1}$ -azide bridged half condensed Schiff base dimers are summarized in Table 4. The observed magnetic behaviour of **1** is in accordance with the behaviour of reported systems.

Complex **2** was found to be diamagnetic, in agreement with the low spin configuration for Co(III) in such an octahedral coordination sphere.

Table 4. Structural and magnetic parameters of reported double $\mu_{1,1}$ - N_3 bridged half condensed Schiff base copper(II) complexes.

S. No.	Compound	Ligand	Cu-Cu Å	Cu-N _{azido} (basal) Å	Cu-N _{azido} (apical) Å	Cu-N-Cu (°)	J ₁ cm ⁻¹	Geometry around Cu(II)
1	[CuL(μ _{1,1} -N ₃) ₂] [*]	 (E)-2-(((2-aminoethyl)imino)methyl)-4-chlorophenol	3.1593(11)	1.949(2) and 2.005(2)	2.001(2) and 2.470(2)	89.30(8)	-2.93(3)	dist. Sq. Py
2	[Cu ₂ (L1) ₂ (N ₃) ₂] ^{5a}	 1-(N-salicylideneamino)-2-aminoethane	3.1807(9)	1.998	2.505(3)	89.1	-8.5(5)	dist. Sq. Py
3	[Cu ₂ (L2) ₂ (N ₃) ₂] ^{5b}	 N-(3-aminopropyl)salicylaldehyde	3.193	2.039(7)	2.440(7)	90.50	-1.8	tri. dist. Sq. Py
4	[Cu ₂ (L3) ₂ (N ₃) ₂] ^{5b}	 7-amino-4-methyl-5-azahept-3-en-2-one	3.161	2.020(4)	2.546(5)	86.82	-3.1	tri. dist. Sq. Py
5	[Cu ₂ (L4) ₂ (N ₃) ₂] ^{5b}	 8-amino-4-methyl-5-azaoct-3-en-2-one	3.318	2.060(8)	2.475(9)	93.60	+2.9	tri. dist. Sq. Py
6	[Cu(L5)(μ _{1,1} -N ₃) ₂] ^{13b}	 (E)-2-(((2-aminoethyl)imino)methyl)-6-ethoxyphenol	3.1208(5)	1.984(18)	2.489(19)	87.71(7)	-10.16	dist. Sq. Py

7	$[\text{Cu}(\text{L6})(\mu_{1,1}\text{-N}_3)]_2$ ^{13b}	 (E)-2-((2-aminocyclohexyl)imino)methylphenol	3.227(2)	2.005(5)	2.5005(5)	90.83(18)	-4.18	dist. Sq. Py
8	$[\text{Cu}(\text{L7})(\mu_{1,1}\text{-N}_3)]_2$ ^{13b}	 (E)-2-((2-aminocyclohexyl)imino)methyl-6-ethoxyphenol	3.070(17)	1.983(5)	2.551(6)	84.3(2)	-1.43	dist. Sq. Py
9	$[\text{Cu}_2(\text{L8})_2(\text{N}_3)_2] \cdot \text{DMF}$ ³⁵	 1-((2-aminopropyl)imino)methyl)naphthalen-2-ol	3.1785(8), 3.1822(7)	1.984(4), 1.995(3)	2.646(4), 2.577(4)	85.4(1), 87.2(1)	+9.6	dist. Sq. Py

Note: Superscript indicates the reference number.

*Present complex **1**, dist. Sq. py = distorted square pyramid, tri. dist. Sq. py = trigonally distorted square pyramid.

7. Conclusions

The nature of Schiff base formed (fully or half condensed) with its differing ligating characteristics (tetra- or tridentate) can modify the coordination geometry of the metal ion and in association with auxiliary ligands like azide or thiocyanate, may have important implications on the magnetic behaviour. Previously we've demonstrated the formation of tetranuclear clusters of Cu(II) involving salpn/salophen as Schiff base and azide as an auxiliary ligand.^[18] To observe the role of chloro substituent on the aldehyde of the Schiff base, on the structural changes and associated magnetic properties, our attempts have resulted in the isolation of title complexes templated by metal ion, in which the Schiff base is only half condensed, irrespective of amine to aldehyde molar ratios. Complex **1** is an asymmetric $\mu_{-1,1}$ azide bridged dimer displaying weak antiferromagnetic interactions ($J = -2.93 \text{ cm}^{-1}$), in agreement with the axial-equatorial N_3^- -linkage between the two copper centres. Complex **2** is a monomer of low spin Co(III), as evidenced by structure and cyclic voltammetry studies. These examples provide a direction towards deliberate synthesis of half condensed Schiff base complexes and further investigation on the preparation of half condensed Schiff base complexes by modifying aldehyde and amine environments as well as the nature of metal ions in templating the SB formation are in progress.

Appendix A. Supplementary data

Supplementary data includes IR spectra of complexes **1** and **2** in Figure S1. The 2D fingerprint plot of Hirshfeld is presented as Figure S2. Cyclic voltammogram of complex **2** is shown as Figure S3. CCDC Nos. 1875686-1875687 contains supplementary crystallographic data for complexes **1** and **2** respectively. These data can be obtained free of charge via <http://www.ccdc.cam.ac.uk/conts/retrieving.html>, or from the Cambridge Crystallographic Data Centre, 12 Union Road, Cambridge CB2 1EZ, UK; fax: (+44) 1123-336-033; or e-mail: deposit@ccdc.cam.ac.uk.

Conflicts of interest:

There are no conflicts of interest to declare.

Acknowledgements

Financial assistance from DST, New Delhi, India for the project YSS/2015/000993 is gratefully acknowledged. Prof. Hiroshi Nishihara's laboratory at The University of Tokyo, Tokyo, Japan for the X-ray data of **1** and Department of Chemistry, IIT Kanpur, India is gratefully acknowledged for the X-ray data of **2**. SSS thanks the JSPS, Japan for the bridge fellowship for the visit to Prof. Hiroshi Nishihara's laboratory at The University of Tokyo, Tokyo, Japan.

Keywords: Half condensed Schiff base complexes, Cu(II) & Co(III), Azide, structure, magnetic properties

References:

- [1].(a) J. Schmid, W. Frey, R. Peters, *Organometallics*, 36 (2017) 4313–4324; (b) X. Zhang, Y. Zhu, X. Zheng, D. Phillips, C. Zhao, *Inorg. Chem.*, 53 (2014) 3354–3361; (c) A. Bhattacharjee, S. Halder, K. Ghosh, C. Rizzoli, P. Roy, *New J. Chem.*, 41 (2017) 5696–5706; (d) I. Bratko, M. Gómez, *Dalton Trans.*, 42 (2013) 10664–10681.
- [2]. (a) Z. Gu, J. Na, B. Wang, H. Xiao, Z. Li, *CrystEngComm.*, 13 (2011) 6415–6421; (b) Z. Meng, L. Yun, W. Zhang, C. Hong, R. Herchel, Y. Ou, J. Leng, M. Peng, Z. Lin, M. Tong, *Dalton Trans.*, 0 (2009) 10284–10295; (c) H. Zhang, C. Xue, J. Shi, H. Liu, Y. Dong, Z. Zhao, D. Zhang, J. Jiang, *Cryst. Growth Des.*, 16 (2016) 5753–5761; (d) A. Escuer, J. Esteban, S. Perlepes, T. Stamatatos, *Coord. Chem. Rev.*, 275 (2014) 87–129; (e) C. Maxim, F. Tuna, A. Madalan, N. Avarvari, M. Andruh, *Cryst. Growth Des.*, 12 (2012) 1654–1665.
- [3].(a) Y. Han, N. Chilton, M. Li, C. Huang, H. Xu, H. Hou, B. Moubaraki, S. Langley, S. Batten, Y. Fan, K. Murray, *Chem. Eur. J.*, 19 (2013) 6321–6328; (b) A. Casini, B. Woods, M. Wenzel, *Inorg. Chem.*, 56 (2017) 14715–14729; (c) L. Huo, L. Gao, J. Gao, F. An, X. Niu, T. Hu, *Inorg. Chem. Commun.*, 89 (2018) 83–88; (d) M. Zhang, T. Fan, Q. Wang, H. Han, X. Li, *J. Solid State Chem.*, 258 (2018) 744–752; (e) F. Yuan, C. Yuan, H. Hu, T. Wang, C. Zhou, *J.*

Solid State Chem., 258 (2018) 588–601.

- [4]. (a) M. Chen, M. Chen, C. Zhou, W. Lin, J. Chen, W. Chen, Z. Jiang, *Inorg. Chim. Acta.*, 405 (2013) 461–469; (b) J. Chen, W. Lin, C. Zhou, L. Yau, J. Wang, B. Wang, W. Chen, Z. Jiang, *Inorg. Chim. Acta.*, 376 (2011) 389–395.
- [5]. (a) S. Koner, S. Saha, T. Mallah, K. Okamoto, *Inorg. Chem.*, 43 (2004) 840–842; (b) M. Ray, A. Ghosh, R. Bhattacharya, G. Mukhopadhyay, M. Drew, J. Ribas, *Dalton Trans.* (2004) 252–259.
- [6]. (a) M. Sarkar, R. Clérac, C. Mathonière, N. Hearn, V. Bertolasi, D. Ray, *Inorg. Chem.*, 50 (2011) 3922–3933; (b) S. Biswas, S. Naiya, C. Gómez-García, A. Ghosh, *Dalton Trans.*, 41 (2012) 462–473.
- [7]. (a) Y. Zeng, J. Zhao, B. Hu, X. Hu, F. Liu, J. Ribas, J. Ribas-Ariño, X. Bu, *Chem. Eur. J.*, 13 (2007) 9924–9930; (b) A. Bartyzel, *Polyhedron*, 134 (2017) 30–40; (c) Song, K. Lim, D. Ryu, S. Yoon, B. Suh, C. Hong, *Inorg. Chem.*, 53 (2014) 7936–7940.
- [8]. (a) P. Mukherjee, M. Drew, A. Ghosh, *Eur. J. Inorg. Chem.*, (2008) 3372–3381; (b) A. D. Khalaji, S. Triki, *Russ J. Coord. Chem.*, 38 (2012) 579–582; (c) A. Khalaji, H. Stoekli-Evans, *Polyhedron*, 28 (2009) 3769–3773.
- [9]. (a) M. Ray, A. Ghosh, S. Chaudhuri, M. Drew, J. Ribas, *Eur. J. Inorg. Chem.*, (2004) 3110–3117; (b) R. Hui, P. Zhou, Z. You, *Russ. J. Coord. Chem.*, 36 (2010) 525–529; (c) J. Zhang, X. Zhou, X. Wang, X. Li, Z. You, *Transition Met. Chem.*, 36 (2011) 93–98.
- [10]. S. Jana, B. Shaw, P. Bhowmik, K. Harms, M. Drew, S. Chattopadhyay, S. Saha, *Inorg. Chem.*, 53 (2014) 8723–8734.
- [11]. (a) N. Zare, A. Zabardasti, M. Dusek, V. Eigner, *J. Mol. Struct.*, 1163 (2018) 388–396; (b) M. Kalhor, Z. Seyedzade, *Res. Chem. Intermed.*, 43 (2017) 3349–3360.
- [12]. (a) J. Costes, C. Duhayan, L. Vendier, *Polyhedron*, 153 (2018) 158–162 ; (b) V. Béreau, S. Dhers, J. P. Costes, C. Duhayan, J. P. Sutter, *Eur. J. Inorg. Chem.* (2018) 66-73.
- [13]. (a) P. Bhowmik, S. Jana, S. Chattopadhyay, *Polyhedron*, 44 (2012) 11–17; (b) S. Mondal,

- P. Chakraborty, N. Aliaga-Alcalde, S. Mohanta, *Polyhedron*, 63 (2013) 96–102.
- [14]. (a) R. C. Elder, *Aust. J. Chem.*, 31 (1978) 35-45; (b) S. Naiya, H. Wang, M. Drew, Y. Song, A. Ghosh, *Dalton Trans.*, 40 (2011) 2744–2756.
- [15]. (a) S. Koner, S. Saha, K. Okamoto, J. Tuchagues, *Inorg. Chem.*, 42 (2003) 4668–4672; (b) I. Pankov, I. Shcherbakov, V. Tkachev, S. Levchenkov, L. Popov, V. Lukov, S. Aldoshin, V. Kogan, *Polyhedron*, 135 (2017) 237–246.
- [16]. (a) S. Mukherjee, P. Mukherjee, *Cryst. Growth Des.* 14 (2014) 4177–4186; (b) S. Naiya, C. Biswas, M. Drew, C. Gómez-García, J. Clemente-Juan, A. Ghosh, *Inorg. Chem.*, 49 (2010) 6616–6627; (c) S. Majumder, S. Sarkar, S. Sasmal, E. Sañudo, S. Mohanta, *Inorg. Chem.*, 50 (2011) 7540–7554.
- [17]. (a) P. Seth, S. Ghosh, A. Figuerola, A. Ghosh, *Dalton Trans.*, 43 (2014) 990–998; (b) B. K. Babu, A. R. Biju, S. Sunkari, M. V. Rajasekharan, J. Tuchagues, *Eur. J. Inorg. Chem.*, (2013) 1444–1450.
- [18]. P. Pandey, N. Dwivedi, G. Cosquer, M. Yamashita, S. Sunkari, *ChemistrySelect*, 3 (2018) 10311–10319.
- [19]. S. Sahadevan, E. Cadoni, N. Monni, C. Pipaón, J. Mascaros, A. Abhervé, N. Avarvari, L. Marchiò, M. Arca, M. Mercuri, *Cryst. Growth Des.*, 18 (2018) 4187–4199.
- [20]. S. Jana, B. Shaw, P. Bhowmik, K. Harms, M. Drew, S. Chattopadhyay, S. Saha, *Inorg. Chem.*, 53 (2014) 8723–8734.
- [21]. G. M. Sheldrick, *Acta Cryst. A.*, 64 (2008) 112–122.
- [22]. M. N. Burnett, C. K. Johnson, Report ORNL–6895. Oak Ridge National Laboratory, Oak Ridge, Tennessee, (1996).
- [23]. I. J. Bruno, J. C. Cole, P. R. Edgington, M. K. Kessler, C. F. Macrae, P. McCabe, J. Pearson, R. Taylor, *Acta Cryst. B.*, 58 (2002) 389–397.
- [24]. S. K. Wolff, D. J. Grimwood, J. J. McKinnon, D. Jayatilaka, M. A. Spackman, Crystal Explorer 2.1, University of Western Australia, Perth, Australia, (2007).

- [25]. (a) M. S. Ray, A. Ghosh, S. Chaudhuri, M. G. B. Drew, J. Ribas, *Eur. J. Inorg. Chem.*, (2004) 3110–3117; (b) M. Zbiri, S. Saha, C. Adhikary, S. Chaudhuri, C. Daul, S. Koner, *Inorg. Chim. Acta.*, 359 (2006) 1193–1199.
- [26]. (a) P. Pandey, B. Kharediya, B. Elrez, J.-P. Sutter, S. Sunkari, *J. Coord. Chem.*, 70 (2017) 1237–1246; (b) P. Pandey, B. Kharediya, B. Elrez, J.-P. Sutter, G. Bhargavi, M. V. Rajasekharan, S. Sunkari, *Dalton Trans.*, 46 (2017) 15908–15918.
- [27] Z. You, Q. Jiao, S. Niu, J. Chi, *Z. Anorg. Allg. Chem.*, 632 (2006) 2481–2485.
- [28] N. Salem, A. Rashad, L. El Sayed, W. Haase, M. Iskander, *Polyhedron*, 68 (2014) 164–171.
- [29] K. Azouzi, B. Hamdi, R. Zouari, A. Ben Salah, *Ionics*, 22 (2016) 1669–1680.
- [30] (a) N. Dwivedi, S. Panja, Monika, S. Saha, S. Sunkari, *Dalton Trans.*, 45 (2016) 12053–12068; (b) M. Masoudi, M. Behzad, A. Arab, A. Tarahhomi, H. A. Rudbari, G. Bruno, *J. Mol. Struct.*, 1122 (2016) 123–133; (c) I. Kodrin, Ž. Soldin, C. Aakeröy, M. Đaković, *Cryst. Growth Des.* 16 (2016) 2040–2051.
- [31] (a) M. Sarkar, R. Clérac, C. Mathonière, N. G. R. Hearn, V. Bertolasi, D. Ray, *Inorg. Chem.*, 49 (2010) 6575–6585; (b) E. Lalinde, R. Lara, I. P. Lójepez, M. T. Moreno, E. Alfaro-Arnedo, J. G. Pichel, S. Piñero-Hermida, *Chem. Eur. J.*, 24 (2018) 2440–2456; (c) X. Zhu, P. Cui, S. Kilina, W. Sun, *Inorg. Chem.*, 56 (2017) 13715–13731.
- [32] Y. Zeng, X. Hu, F. Liu, X. Bu, *Chem. Soc. Rev.*, 38 (2009) 469–480.
- [33] (a) B. Bleaney, K. D. Bowers, *Proc. R. Soc. London, Ser. A*, 214 (1952) 451. (b) O. Kahn, *Molecular Magnetism*, VCH, Weinheim, (1993) 104.
- [34] N. F. Chilton, R. P. Anderson, L. D. Turner, A. Soncini, K. S. Murray, *J. Comput. Chem.* 34 (2013) 116–1175.
- [35] S. Jana, B. Shaw, P. Bhowmik, K. Harms, M. Drew, S. Chattopadhyay, S. Saha, *Inorg. Chem.*, 53 (2014) 8723–8734.

SUPPORTING INFORMATION

Figure S1. IR Spectra of complexes **1** and **2**.

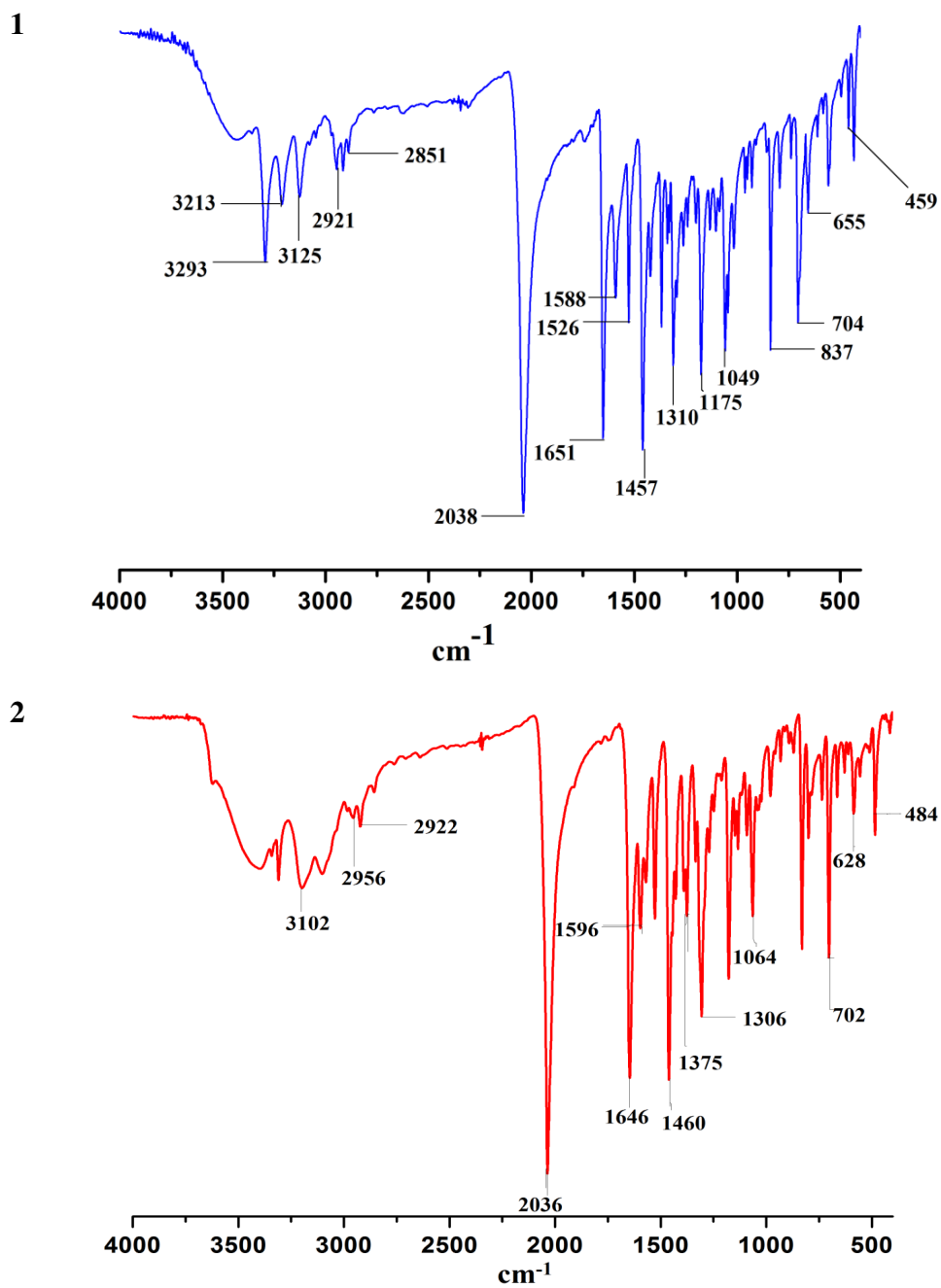
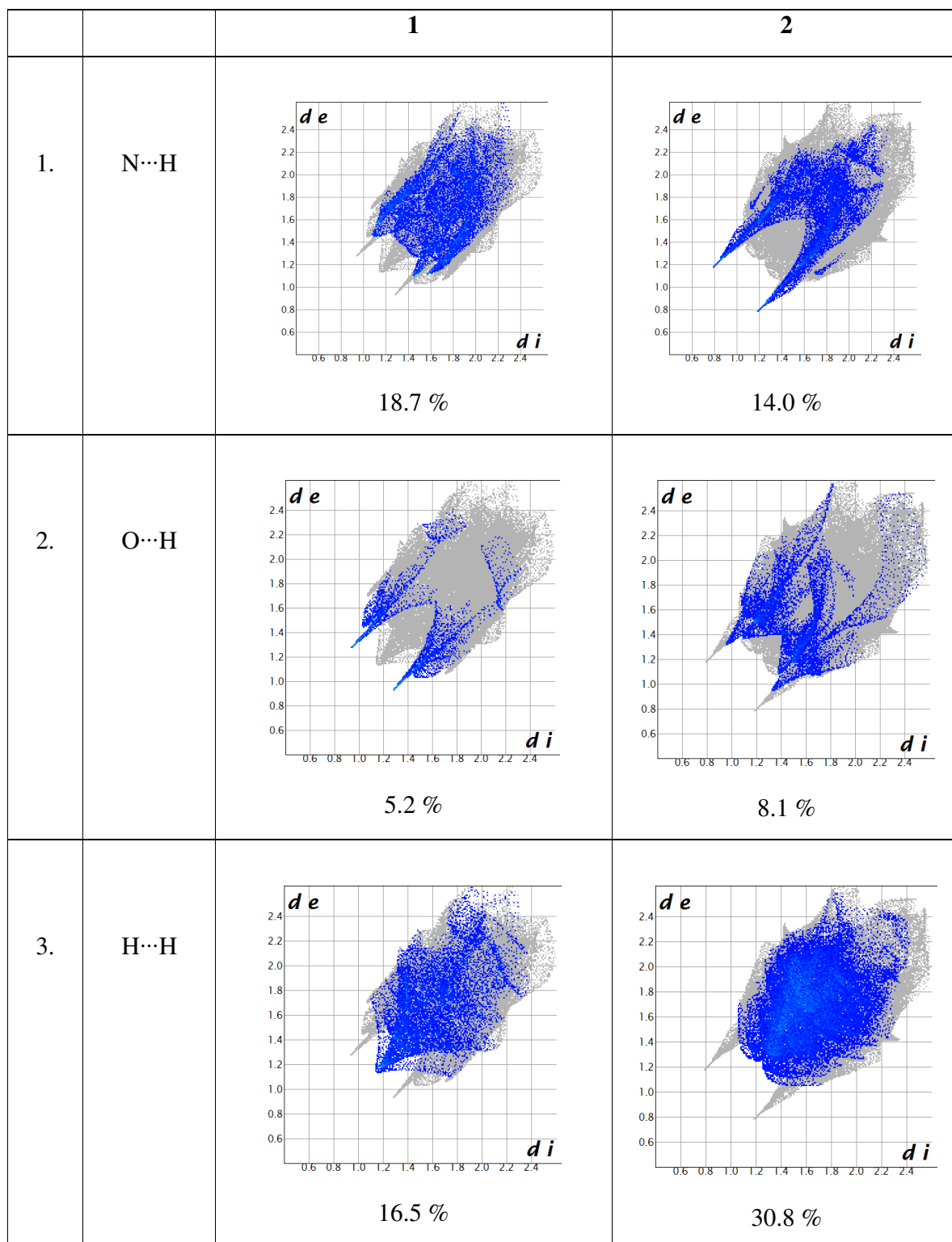
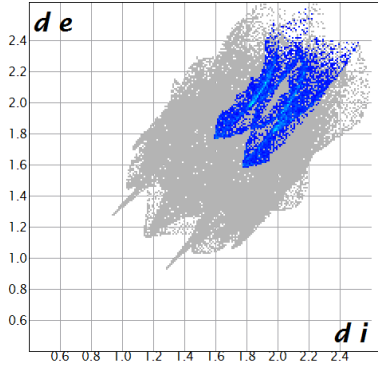
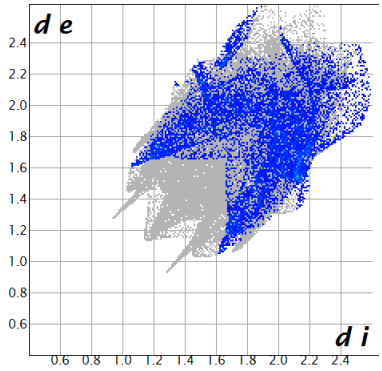
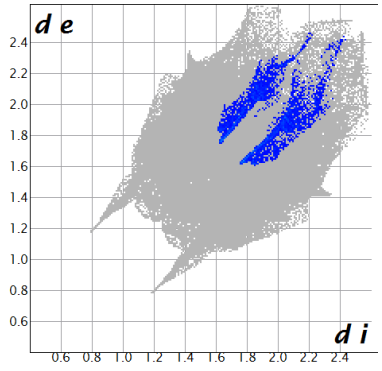
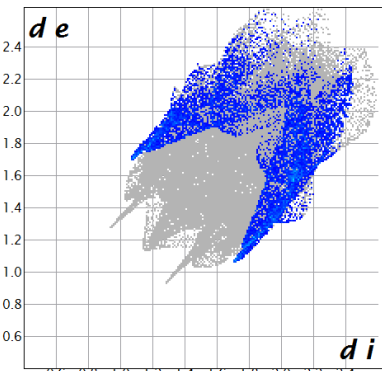
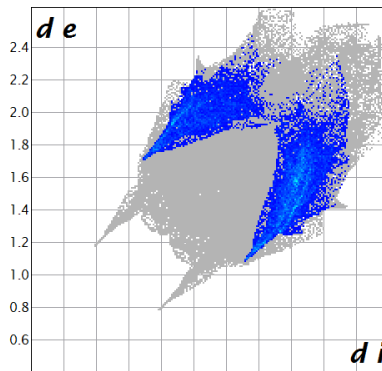
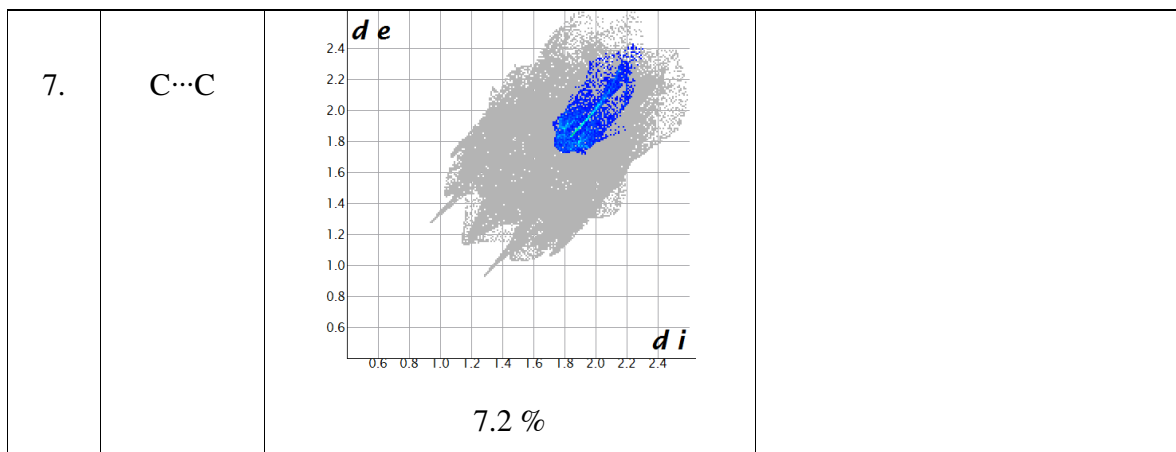


Figure S2. The Hirshfeld 2D fingerprint plots of **1** and **2**.



4.	C...N	 <p data-bbox="662 728 758 772">9.2 %</p>	
5.	C...H	 <p data-bbox="662 1232 758 1276">16.3 %</p>	 <p data-bbox="1125 1232 1220 1276">3.2 %</p>
6.	Cl...H	 <p data-bbox="662 1747 758 1792">12.8 %</p>	 <p data-bbox="1125 1747 1220 1792">16.3 %</p>



8. Cyclic voltammetric studies

The cyclic voltammetric study for the monomeric cobalt complex **2** was performed in phosphate buffer (pH=7) as shown in Figure S3. Three electrode assembly was utilized (bare GCE, glassy carbon electrode was used as a working electrode, Pt electrode as an auxillary electrode, Ag/AgCl as a reference electrode). Cyclic voltammogram of cobalt complex was scanned with in potential window of -1.25 to 0.5 volt at scan rate 200 mv/s shows electrochemically irreversible one step $1 \bar{e}$ reduction process for Co(III)/ Co(II) at -0.914 V.^[S1]

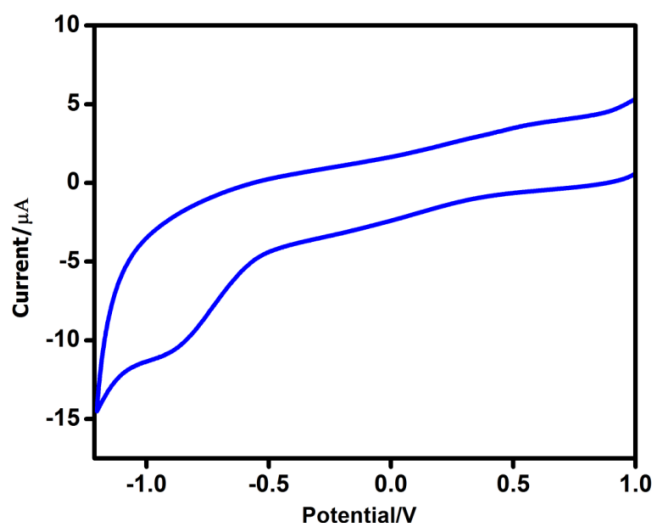


Figure S3. Cyclic voltammogram of complex **2** at a scan rate of 200 mV/s.

Fig-S4: Curie-Weiss analysis of $\chi_M^{-1} = f(T)$; χ_M is per Cu center and fit was performed for data above 20 K. Best fit parameters are given in the plot.

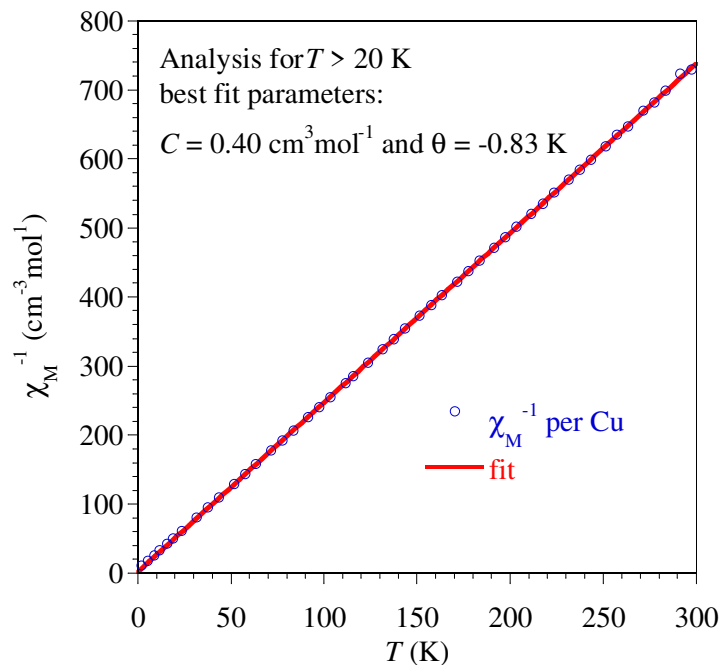
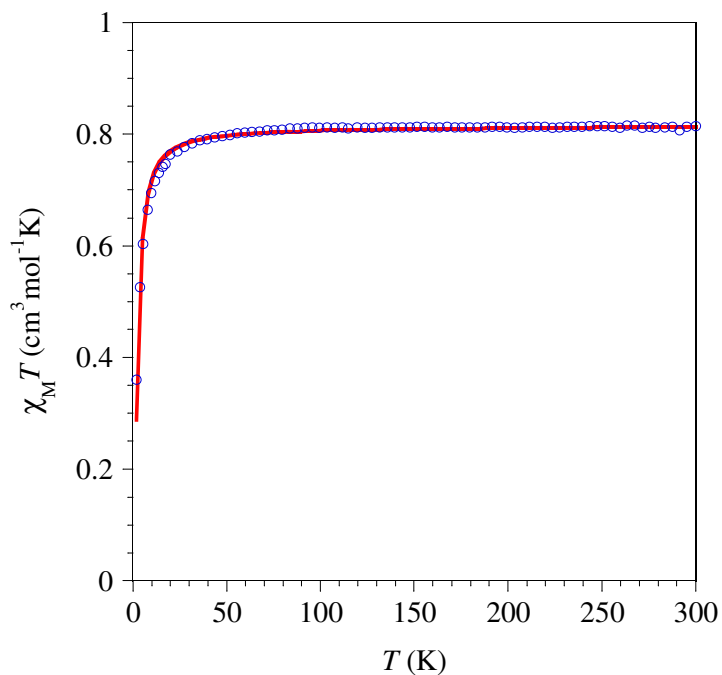


Fig. S5: Experimental (\square) temperature dependence of cMT for **1** with best fit (—) of the Bleaney-Bowers expression for a dimer of $S = \frac{1}{2}$ spins derived from the phenomenological Hamiltonian $H = -J\mathbf{S}_A \cdot \mathbf{S}_B$. Best fit parameters: $J = -2.93 \pm 0.03 \text{ cm}^{-1}$ and $g = 2.084 \pm 0.001$



References:

[S1] (a) P. Pandey, G. Cosquer, M. Yamashita, S. S. Sunkari, *ChemistrySelect*, **2018**, 3, 2240 – 2244; (b) S. Meghdadi, K. Mereiter, M. Amrinasr, F. Fadaee, A. Amiri, *J. Coord. Chem.* **2009** 62, 734 -744.